

## Influence of Laser Irradiation on the Constant Composition Kinetics of Enamel Dissolution

D.E. Gerard<sup>a</sup> D. Fried<sup>b</sup> J.D.B. Featherstone<sup>b</sup> G.H. Nancollas<sup>a</sup>

<sup>a</sup>University at Buffalo, The State University of New York, Buffalo, N.Y., and <sup>b</sup>University of California at San Francisco, San Francisco, Calif., USA

### Key Words

Constant composition · Dental enamel · Dissolution kinetics · Laser irradiation

### Abstract

The influence of 9.6  $\mu\text{m}$   $\text{CO}_2$  laser irradiation on enamel dissolution kinetics was investigated using a constant composition method designed for rate measurements of enamel dissolution as a function of depth, on a micrometer scale. In contrast to lower irradiation intensities ( $\leq 1.0 \text{ J cm}^{-2}$ ), which consistently showed reduced dissolution rates, higher fluences (energy per surface area) resulted in initially increased dissolution rates, which rapidly decreased, after dissolution times corresponding to removal of a few micrometers, to rates similar to those acquired using lower fluences. It was also demonstrated that surface damage during laser irradiation could be limited to the first 1–2  $\mu\text{m}$  by lowering the number of pulses per spot during the irradiation procedure. The constant composition method can be used to measure detailed kinetics of inhibition of acid dissolution of dental enamel that has been treated by low fluence 9.6- $\mu\text{m}$   $\text{CO}_2$  laser irradiation.

Copyright © 2005 S. Karger AG, Basel

The use of lasers for dental applications, first introduced over 35 years ago, has been extensively evaluated for both soft and hard tissues. High-energy ruby lasers, originally tested for their effects on enamel and dentin, produced craters in enamel surfaces and decreased permeability through surface fusion [Myers, 1991]. However, high fluences (energy/surface area) were required, which resulted in elevated temperatures throughout the samples and undesirable effects, such as cracking, pitting and pulpal damage.  $\text{CO}_2$  lasers, which emit in the IR region, proved equally effective without any significant damaging side effects, provided care was taken to maintain temperatures at a safe level. Temperature changes within the pulp chamber exceeding 5°C could result in permanent damage to the dental pulp [Zach and Cohen, 1965].

Optimal irradiation conditions call for wavelengths strongly absorbed by the components of the tissue such that light scattering is negligible. For dental enamel, which is primarily carbonated apatite with ~5% by weight of water and organic matrix, several absorption bands occur between 2 and 11  $\mu\text{m}$  in the IR region. Water has a broad absorption band centered at about wavelength ( $\lambda$ ) = 3.0  $\mu\text{m}$ , while the hydroxyl groups in both water and apatite absorb at 2.8  $\mu\text{m}$ . Energy is absorbed most efficiently by the apatite phosphate groups through the three P–O stretching modes at wavelengths of 9.2, 9.6, and 10.4  $\mu\text{m}$  [Fowler et al., 1966; Kravitz et al., 1968; Fowler, 1974].

Ablation is most efficient if the pulse duration (PD) is less than the thermal relaxation time of the mineral (the time taken for the majority of the energy to be transformed into heat). The shorter the pulse duration the more localized the heat distribution, whereas longer durations would unnecessarily distribute energy deeper into the tissue [Seka et al., 1996; Featherstone et al., 1998a, b].

The primary use of lasers in hard tissue dentistry has been for the removal of carious tissue through ablation and the FDA has approved the use of Er:YAG ( $\lambda = 2.94 \mu\text{m}$ ) and Er:YSGG ( $\lambda = 2.79 \mu\text{m}$ ) lasers for the removal of tissue by heating subsurface water, causing ablation [Fried et al., 1996]. Another potential use of lasers involves the treatment of enamel or dentin to render the surfaces more resistant to locally produced acids by either altering the composition of the mineral phase and/or decreasing the permeability, thus decreasing access of acid to the interior [Featherstone et al., 1998a, b].

Through the application of laser energy, the mineral composition may be altered by expelling carbonate (400–600°C), thereby improving the crystallinity, which may be further improved by sintering the tissue at 800°C, to increase crystal dimensions to as much as 10 times their original size [McCormack et al., 1995; Fried et al., 1998]. The permeability may also be decreased by heating the mineral to temperatures between 800–900°C, near the early stages of melting, in order to fuse the crystals slightly without damaging the crystal integrity. This was demonstrated by Kawasaki et al. [2000], using a pulsed 9.6- $\mu\text{m}$  CO<sub>2</sub> laser to decrease surface porosity.

Since desirable thermally induced changes occur at or below 900°C, it was suggested [Featherstone et al., 1998a, b; Featherstone and Fried, 2001] that the ideal laser irradiation temperatures should be around 800–900°C, taking care not to greatly exceed 900°C. Temperatures above 1,200°C result in apatite melting, which not only decreases the crystallinity, but may also lead to the formation of more soluble calcium phosphate phases such as tetracalcium diphosphate (TTCP) and tricalcium phosphate (TCP) which, although not stable at high temperatures, may remain after transient temperature rises [Nelson et al., 1987].

The aim of the present study was to use a constant composition dissolution method to study in detail the potential acid resistance imparted to dental enamel by irradiation with low fluences of laser light at 9.6  $\mu\text{m}$ , the wavelength most strongly absorbed by dental enamel. Several previous studies have shown this to be effective in inhibiting the progression of artificial subsurface dental caries in human enamel [Featherstone et al., 1998; Featherstone

and Fried, 2001]. We chose to examine in detail the surface dissolution rates under constant composition conditions of dental enamel to eliminate the complication of subsurface diffusion and thereby provide direct information about the mechanism of dissolution inhibition by laser irradiation. Our previous studies [Featherstone et al., 1998] used a pulse duration of 100  $\mu\text{s}$  and showed inhibition of subsurface lesion progression with irradiation intensities of 1.25, 2.5 and 5.0 J cm<sup>-2</sup>, with better results at 2.5 and 5.0. Therefore we used a fluence of 3.0 J cm<sup>-2</sup> and pulse duration of 100  $\mu\text{s}$  as one of our sets of conditions in the present study.

Recent work has examined the use of shorter pulse durations closer to the thermal relaxation time (approximately 1–2  $\mu\text{s}$ ) of dental enamel at this wavelength since more efficient ablation can be achieved [Fried et al., 2001]. Ideally, conditions that could be used for both ablation and for reduction of enamel solubility would be most useful clinically. We found that best ablation conditions were achieved by using pulse durations of 5–8  $\mu\text{s}$  as this produced less plasma formation and efficient ablation [Fried et al., 2001]. In this study examination of surfaces by FTIR analysis also showed that with a pulse duration of 2  $\mu\text{s}$  almost total removal of carbonate from the carbonated apatite mineral was achieved with a fluence of 0.5–1.0 J cm<sup>-2</sup>, which should logically translate into reduced acid solubility. Therefore in the present study we examined pulse durations of 5 and 8  $\mu\text{s}$  together with varying fluences of 0.5, 1.0, 1.5 and 3.0 J cm<sup>-2</sup>. Further, we expected that by using a pulse duration intermediate between 5 and 100  $\mu\text{s}$  we would achieve the best compromise between ablation possibilities (with a high fluence) and inhibition of acid dissolution. We therefore included pulse durations of 20 and 100  $\mu\text{s}$ .

## Materials and Methods

### *Laser Irradiation Conditions*

All laser irradiation was carried out at a wavelength of 9.6  $\mu\text{m}$ . For pulse durations of 5 and 8  $\mu\text{s}$  we used a custom-built 9.6- $\mu\text{m}$ -long pulsed TEA carbon dioxide laser (Argus Photonics Group, Jupiter, Fla., USA) with a special gas mixture to produce a stretched pulse. Fluences used for these conditions were 0.5, 1.0, 1.5 and 3.0 J cm<sup>-2</sup>. For the 20- and 100- $\mu\text{s}$  pulse durations we used carbon dioxide lasers from Pulse Systems Inc. (N. Mex., USA). The pulse duration of approximately 20  $\mu\text{s}$ , which when measured had a tail to about 30  $\mu\text{s}$ , will be termed a 20- to 30- $\mu\text{s}$  pulse duration, and for this condition we used fluences of 1.0 and 2.0 J cm<sup>-2</sup>, expecting the best conditions to be intermediate between the two boundaries described above for longer and shorter pulse durations. The full set of laser irradiation conditions is listed in table 1.

**Table 1.** Dissolution rates, averaged for 2–3 replicates, for each set of laser irradiation conditions

	Fluence J cm <sup>-2</sup>	Pulse duration <sup>1</sup> , μs	Pulses per spot	Initial rate 10 <sup>-2</sup> μm/min	Final rate 10 <sup>-2</sup> μm/min
Control	NA	NA		1.65 ± 0.01	1.65 ± 0.01
A-1.0	1.0	20–30	25	1.26 ± 0.33	1.26 ± 0.33
A-2.0	2.0	20–30	25	3.32 ± 0.55	0.724 ± 0.04
A-3.0	3.0	100	25	4.75 ± 0.47	0.741 ± 0.09
B-0.5	0.5	5	25	1.40 ± 0.13	1.40 ± 0.13
B-1.0	1.0	5	25	1.01 ± 0.54	1.01 ± 0.54
C-0.5	0.5	8	10	0.975 ± 0.08	0.975 ± 0.08
C-1.0	1.0	8	10	0.823 ± 0.22	0.823 ± 0.22
C-1.5	1.5	8	10	2.66 ± 0.36	0.866 ± 0.15
C-3.0	3.0	8	10	2.25 ± 0.24	0.764 ± 0.08

NA = Not assessed. All samples irradiated at wavelength of 9.6 μm with the exception of the control samples, which were not lased.

<sup>1</sup> Pulse durations of 5–8 and 20–100 μs were attained using an ARGUS and PSI CO<sub>2</sub> laser, respectively.

Bovine enamel blocks 4 mm × 4 mm were prepared as described previously [Fried et al., 2002] from bovine incisors, cementum removed, and the enamel surface serially polished to a 1-μm finish. Each block was irradiated with one of each of the above sets of conditions with either 10 or 25 pulses per spot, a repetition rate of 10 Hz, with a 1-mm diameter beam and with spots overlapping at 250-μm intervals to give complete coverage of the surface. Three blocks were prepared for each set of conditions.

The enamel samples were painted with an acid-resistant varnish, so as to expose to the dissolution media only the laser-irradiated surfaces (4 mm × 4 mm) having a total surface area of the 0.16 cm<sup>2</sup>. For this study, dissolution was monitored using a constant composition method specifically designed for very small surface areas. The precision of the technique allowed for the monitoring of changes in dissolution rates as a function of depth at less than 1-μm intervals.

#### Constant Composition Dissolution

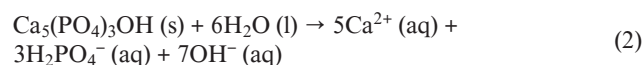
Undersaturated solutions were prepared in 65-ml double-walled cells, thermostated, at 37.0 ± 0.1°C, by mixing calcium chloride, T<sub>Ca</sub> = 3.30 mM, and potassium dihydrogen phosphate, T<sub>P</sub> = 1.98 mM, where T<sub>Ca</sub> and T<sub>P</sub> are the total calcium and phosphate concentrations, respectively. The ionic strength was adjusted to 0.15 M, and the pH to 4.50 using sodium chloride and hydrochloric acid, respectively, yielding a relative undersaturation, σ, of -0.72. σ is defined as

$$\sigma = S - 1 = [\text{IP}/K_{\text{sp}}]^{1/n} - 1 \quad (1)$$

where S is the HAP undersaturation ratio, n is the number of ions in a formula unit of the dissolving phase, and IP and K<sub>SP</sub> are the ionic and solubility products, respectively. The value for K<sub>SP</sub> used was 2.35 × 10<sup>-59</sup> [McDowell et al., 1977].

Dissolution experiments were initiated by suspending the irradiated enamel samples in the magnetically stirred dissolution cells and were monitored using the Constant Composition technique [Tomson and Nancollas, 1978; Ebrahimpour et al., 1991]. Dissolution was monitored using an Orion 720A potentiometer with a glass

electrode (Orion No. 91-01) and reference electrode (Orion 90-01). Any increase in pH detected by the electrode triggered the addition of titrant designed to maintain ion activities at their original levels. Titrant concentrations were calculated on the basis of hydroxyapatite (HAP) dissolution at pH = 4.5.



In order to maintain constant activities and pH, the titrant contained NaCl to adjust the ionic strength and hydrochloric acid where [H<sup>+</sup>] = 7/5 T<sub>Ca</sub>. Reaction rates, R<sub>d</sub>, expressed as moles of equivalent HAP dissolved per minute, were calculated using Eq. 3:

$$R_d = 0.143 [\text{H}^+] (dV_t/dt) \quad (3)$$

where (dV<sub>t</sub>/dt) is the volume of titrant added per minute.

Depth of total dissolution, d, was estimated from Eq. 4, assuming an enamel density equal to that of HAP, ρ = 3.15 g cm<sup>-3</sup>,

$$d = (V_t [\text{H}^+] \text{MW})/(\rho A) \quad (4)$$

In Eq. 4, V<sub>t</sub> is the volume of titrant added, A is the area of exposed enamel (0.16 cm<sup>2</sup>), and MW is the molecular weight of HAP.

During the reactions, solution samples were withdrawn and analyzed for total calcium (atomic absorption: Perkin Elmer 3100 spectrophotometer) and phosphate (spectrophotometrically as the vanadomolybdate complex: Varian Cary 210 spectrophotometer) [Tomson et al., 1977] to verify constancy of composition.

## Results

The experimental mean enamel dissolution data are presented in table 1 as initial and final dissolution rates corresponding to the linear portions of the curves in figures 1, 2. The average profiles of moles of equivalent HAP

**Fig. 1.** Average amount of mineral (as HAP) dissolved as a function of time. Pulses per spot = 25; pulse duration (PD) = 5–100  $\mu$ s.

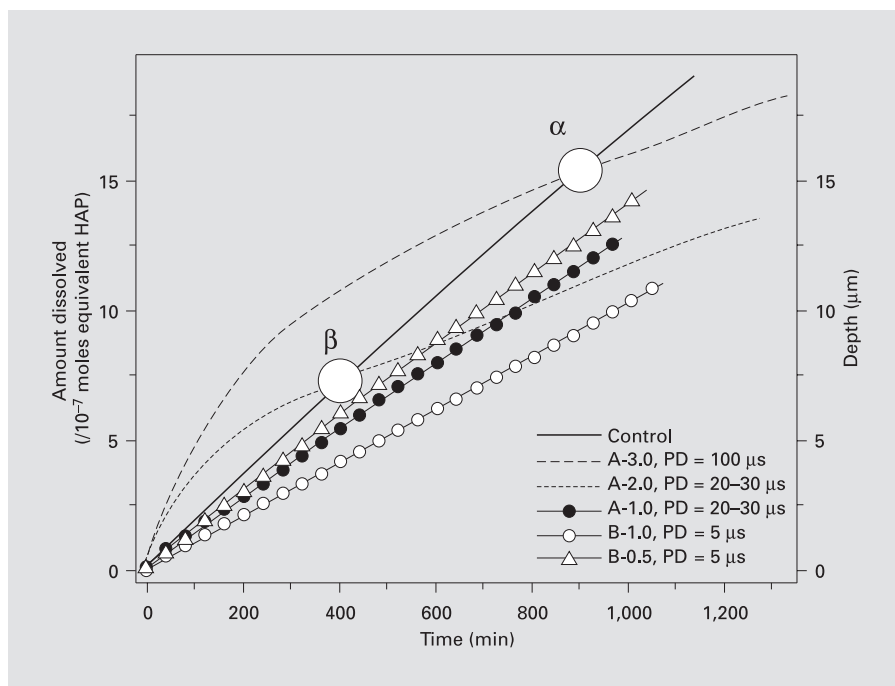
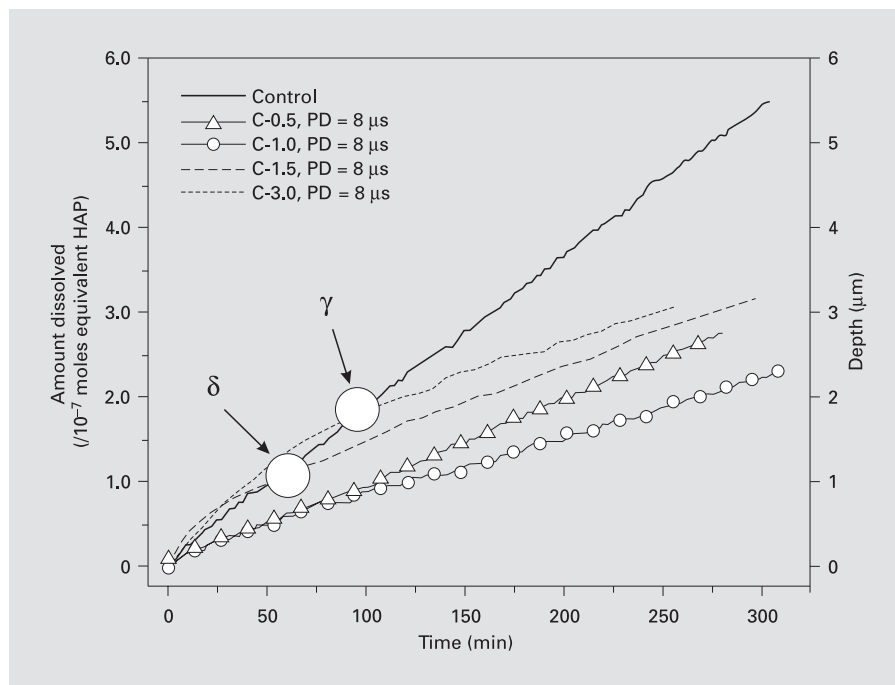


**Fig. 2.** Average amount of mineral (as HAP) dissolved as a function of time. Pulses per spot = 10; pulse duration (PD) = 8  $\mu$ s.



dissolved and depth of dissolution for the irradiation conditions in groups A and B, treated with 25 pulses per spot, are plotted versus time in figure 1. It can be seen that fluences  $\leq 1.0 \text{ J cm}^{-2}$  yielded linear time plots of dissolution rates, but with as much as a 39% decrease in rate compared to the nonirradiated control group. Fluences  $>1.0 \text{ J cm}^{-2}$  resulted in considerably greater initial dissolution rates than the control by a factor of 2–2.5 over depths of several micrometers. These dissolution rates subsequently decreased with time, as the acid dissolved more mineral, until an approximately constant ‘final’ dissolution rate, 44–76% that of the nonirradiated control samples, was achieved.

As described above in the rationale for the choice of irradiation conditions we also investigated a pulse duration of  $8 \mu\text{s}$  with 10 pulses per spot (group C, table 1). Results for group C rates of dissolution are listed in table 1 and the average dissolution profiles are plotted in figure 2.

Dissolution trends for group C were similar to groups A and B, at all fluences  $\leq 1.0 \text{ J cm}^{-2}$  with approximately constant rates that were appreciably less than those for the nonirradiated enamel. Irradiation at fluences  $>1.0 \text{ J cm}^{-2}$  again resulted in initial dissolution rates markedly greater than the control, followed by a steady decrease until rates again were approximately 50% inhibited in comparison with the controls.

Although all samples irradiated at  $1.0 \text{ J cm}^{-2}$  resulted in decreased dissolution rates, those irradiated with pulse durations of  $8 \mu\text{s}$  showed the most inhibitory effect,  $\sim 50\%$ , with  $5\text{-}\mu\text{s}$  inhibition  $\sim 39\%$ , and pulse durations of  $20\text{--}30 \mu\text{s}$  producing inhibition of  $\sim 24\%$ .

We calculated the depths at which the total extents of dissolution were the same as those for the nonirradiated control surfaces. Rapid removal of enamel by the acid was limited to less than  $2 \mu\text{m}$  for group C ( $\gamma$ ,  $\delta$ , fig. 2), whereas the group A samples showed markedly elevated dissolution rates for the first  $7$  and  $15 \mu\text{m}$  for fluences of  $2.0$  and  $3.0 \text{ J cm}^{-2}$ , respectively ( $\alpha$ ,  $\beta$ , fig. 1). Subsequent microscopic examination of fresh samples irradiated under the same conditions showed neatly arranged indentations or pits on the surfaces coinciding with the positioning of overlapping spots during the laser irradiation procedure.

## Discussion

The results of this study are consistent with the thermal measurements and simulations of Zuerlein et al. [1999] for  $9.6\text{-}\mu\text{m}$  laser pulses and our experiments

showed significantly accelerated dissolution rates for enamel irradiated at only  $3.0 \text{ J cm}^{-2}$  at the same pulse duration, and microscopic examination showed surface alteration, pits and deposits.

In a study comparing different pulse durations for the same total energy, McCormack et al. [1995] determined that the longer pulse duration unnecessarily distributed energy deeper into the tissue, barely affecting the surface, whereas short durations led to surface fusion and the formation of large octahedral crystals. It was therefore concluded that greater surface damage should be seen for short pulse durations. Nevertheless, in the present work, samples irradiated with longer pulse durations also showed the most accelerated initial dissolution rates.

The combined effect of pulse per spot and pulse duration is clearly demonstrated by comparing the average dissolution rates listed for all the samples irradiated at  $1.0 \text{ J cm}^{-2}$  (pulse durations  $5$ ,  $8$ , or  $20\text{--}30 \mu\text{s}$ ) shown in table 1. Lowering the pulse duration from  $20\text{--}30$  to  $5 \mu\text{s}$  decreased the dissolution rate by an additional  $15\%$ , whereas the lowering of both pulse duration to  $8 \mu\text{s}$  and pulses per spot to  $10$  further decreased the dissolution rate by more than  $\sim 25\%$ .

If the initial dissolution surges reflected surface damage, the effect of pulses per spot and pulse duration may also be seen by comparing the total surface damage at  $3.0 \text{ J cm}^2$  (fig. 1). This was limited to the first  $2 \mu\text{m}$  for sample C-3.0 as opposed to  $\sim 10 \mu\text{m}$  for sample A-1.0, where net inhibition did not occur for the first  $15 \mu\text{m}$ . The observed rate decrease to  $\sim 50\%$  that of the control with initial rates 2–3 times greater than the control can probably be related to the inherent heat dissipation following surface ablation. It has previously been suggested that the optimal temperature for inhibition of acid dissolution was about  $900^\circ\text{C}$  [Featherstone and Fried, 2001]. Since this is close to the early melting point of enamel it would probably lead to fusing and increased crystallinity [McCormack et al., 1995]. Temperatures exceeding  $900\text{--}1,000^\circ\text{C}$  would result in excessive melting and ablation, but the ensuing temperature decrease as a function of depth would result in temperatures favoring maximum inhibition deeper in the mineral. This appears to be the case for fluences  $>1.0 \text{ J cm}^{-2}$ .

Fluences  $\leq 1.0 \text{ J cm}^{-2}$  gave quite different results. The rates were considerably lower than those of the nonirradiated control samples throughout the dissolution experiments. However, surfaces irradiated at higher fluences gave similar dissolution rates to those of the  $1.0 \text{ J cm}^{-2}$  samples after the initial surge. Since heat dissipation after irradiation at these higher fluences would ultimately re-

sult in optimal temperatures for adventitious fusing and carbonate removal, it may be assumed that the conditions chosen for sample C-1.0 (1.0 J cm<sup>-2</sup>, 8 μs, 10 pps) were the most effective for maximally inhibiting enamel dissolution without incurring surface damage. These procedures may prove critical for inhibition of acid dissolution of enamel for several reasons: (1) improved crystallinity, and therefore, lower mineral solubility, (2) fusion induced

lowering of the specific surface area and (3) inhibition of ionic diffusion through the surface since dental caries is a subsurface dissolution process.

### Acknowledgment

We thank the NIH/NIDCR for support of this work through the grant numbers DE03223 and DE09958.

### References

- Ebrahimpour A, Zhang J, Nancollas GHN: Dual constant composition method and its application to studies of phase transformation and crystallization of mixed phases. *J Crystal Growth* 1991;113:83–91.
- Featherstone JDB, Barrett-Vespone NA, Fried D, Kantorowitz Z, Lofthouse J, Seka W: CO<sub>2</sub> laser inhibition of artificial caries-like lesion progression in dental enamel. *J Dent Res* 1998a;77:1397–1403.
- Featherstone JDB, Fried D: Fundamental interactions of lasers with dental hard tissues. *Med Laser Application* 2001;16:181–194.
- Featherstone JDB, Fried D, Duhn CW: Surface dissolution kinetics of dental hard tissue irradiated over a fluence range of 1–8 J/cm<sup>2</sup>. SPIE, The International Society for Optical Engineering: Proc Lasers in Dentistry IV 1998b; 3248:3248–3221.
- Fowler BO: Infrared studies of apatites. II. Preparation of normal and isotopically substituted calcium, strontium and barium hydroxyapatites and spectra-structure-composition correlations. *Inorg Chem* 1974;13:207–214.
- Fowler BO, Moreno EC, Brown WE: Infra-red spectra of hydroxyapatite, octacalcium phosphate and pyrolyzed octacalcium phosphate. *Arch Oral Biol* 1966;11:477–492.
- Fried D, Ragadio J, Akriovou M, Featherstone JDB, Murray MW, Dickenson KM: Dental hard tissue modification and removal using sealed transverse excited atmospheric-pressure lasers operating at λ = 9.6 and 10.6 micrometers. *J Biomed Opt* 2001;6:231–238.
- Fried D, Visuri SR, Featherstone JDB, Walsh JT, Seka W, Glana RE, McCormack SM, Wigdor HA: Infrared radiometry of dental enamel during Er:YAG and Er:YSGG laser irradiation. *J Biomed Opt* 1996;1:455–465.
- Fried D, Xie J, Shafi S, Featherstone JDB, Breunig CL: Imaging caries lesions and lesion progression with polarization sensitive optical coherence tomography. *J Biomed Opt* 2002;7:618–627.
- Fried D, Zuerlein MJ, Featherstone JDB, Seka W, Duhn CW, McCormack SM: IR laser ablation of dental enamel: Mechanistic dependence on the primary absorber. *Appl Surf Sci* 1998;127–129:852–856.
- Kawasaki K, Tanaka Y, Takagi O: Crystallographic analysis of demineralized human enamel treated by laser-irradiation or remineralization. *Arch Oral Biol* 2000;45:797–804.
- Kravitz LC, Kingsley JD, Elkin EL: Raman and infrared studies of coupled PO<sub>4</sub><sup>3-</sup>vibrations. *J Chem Phys* 1968;49:4600–4610.
- McCormack SM, Fried D, Featherstone JDB, Glana RE, Seka W: Scanning electron microscope observations of CO<sub>2</sub> laser effects on dental enamel. *J Dent Res* 1995;74:1702–1708.
- McDowell H, Gregory TM, Brown WE: Solubility of hydroxyapatite (Ca<sub>5</sub>(PO<sub>4</sub>)<sub>3</sub>OH) in the system calcium hydroxide-phosphoric acid-water at 5, 15, 25, and 37°C. *J Res Natl Bureau Stand, Section A: Physics and Chemistry* 1977; 81A:273–281.
- Myers ML: The effect of laser irradiation on oral tissues. *J Prosthet Dent* 1991;66:395–397.
- Nelson DGA, Wefel JS, Jongebloed WL, Featherstone JDB: Morphology, histology and crystallography of human dental enamel treated with pulsed low energy infrared laser radiation. *Caries Res* 1987;21:411–426.
- Seka W, Featherstone JDB, Fried D, Visuri SR, Walsh JT: Laser ablation of dental hard tissue: From explosive ablation to plasma mediated ablation. SPIE, The International Society for Optical Engineering: Proc Lasers in Dentistry II 1996;2672:144–158.
- Tomson M, Barone JP, Nancollas GH: Precise calcium phosphate determination. *At Absorpt Newsl* 1977; 16: 117.
- Tomson M, Nancollas GHN: Mineralization kinetics: A constant composition approach. *Science* 1978;200:1059–1060.
- Zach L, Cohen G: Pulp responses to externally applied heat. *Oral Surg Oral Med Oral Pathol* 1965;19:515–530.
- Zuerlein MJ, Fried D, Featherstone JDB, Seka W: Optical properties of dental enamel in the mid-IR determined by pulsed photothermal radiometry. *IEEE J Selected Top Quantum Electronics* 1999;5:1083–1089.